Crystalline State Reaction of Cobaloxime Complexes by X-ray Exposure. 1. A Direct Observation of Co–C Bond Cleavage in [(*R*)-1-Cyanoethyl][(*S*)-(−)-α-methylbenzylamine]-bis(dimethylglyoximato)cobalt(III)

Yuji Ohashi,*[1a] Kazunori Yanagi,[1a] Toshiharu Kurihara,[1a] Yoshio Sasada,[1a] and Yoshiaki Ohgo[1b]

Contribution from the Laboratory of Chemistry for Natural Products, Tokyo Institute of Technology, Nagatsuta, Midori-ku, Yokohama 227, Japan, and Niigata College of Pharmacy, 5829 Kamishinei-cho, Niigata 950-21, Japan. *Received March 13, 1981*

Abstract: A crystal of [(*R*)-1-cyanoethyl][(*S*)-(−)-α-methylbenzylamine]bis(dimethylglyoximato)cobalt(III) changes its unit-cell dimensions by X-ray exposure without degradation of a single crystal form. The rate is so slow that three-dimensional intensity data can be obtained at the initial, intermediate, and final stages of the change. The electron density map at every stage proves that the (*R*)-1-cyanoethyl group gradually changed to the disordered racemate so that the complex revealed an epimerization. ESR spectra of the crystal indicate that the Co–C bond is cleaved homolytically by X-ray irradiation. The reaction follows approximate first-order kinetics, the rate constant being 3.3×10^{-6} s^{-1}. At the early stages, the first-order plot is somewhat sigmoidal. Racemization of the cyanoethyl group was no longer detectable below 173 K. Comparison of the two structures at 293 and 173 K indicates that the void space around the cyanoethyl group is essential for the crystalline state reaction.

During serial structure analyses of cobaloxime complexes,[2-6] aimed at interpreting the catalytic capability of the asymmetric hydrogenation,[7-12] we have found that crystals of [(*R*)-1-cyanoethyl][(*S*)-(−)-α-methylbenzylamine]bis(dimethylglyoximato)-cobalt(III) (Figure 1) (hereafter bis(dimethylglyoximato)cobalt is abbreviated to cobaloxime) change their unit-cell dimensions by X-ray exposure without degradation of the crystallinity. The rate of the change was so slow that three-dimensional intensity data were obtained in each stage of the change. By calculating the electron density using the data, we have proved that the change reflects the racemization of the cyanoethyl group. When the crystal was cooled, the rate of the change became slow and the change was no longer detectable below 173 K. Although the racemization of the cyanoethyl group should be mentioned as the epimerization of the complex, the former term is used in the present serial papers to avoid a confusion because similar changes have been observed for the crystals containing the axial ligands of achiral amines.[13]

This paper reports details of these quite new findings of the racemization in the crystalline state and discusses the possible mechanism of the change. Preliminary work has already been reported.[14,15]

Experimental Section

Dark red platelike crystals were obtained by fractional crystallization from an aqueous methanol solution containing the diastereomeric both configuration of the complexes. Details of the preparation have been reported.[16] The crystal was mounted on a Rigaku four-circle diffractometer, the distance between the crystal and focus of X-ray tube being 25 cm. Mo Kα radiation monochromated by graphite was used (50 kV, 30 mA, λ = 0.71069 Å). The unit-cell dimensions were obtained by means of the least-squares technique with 15 reflections in the range of $21° < 2\theta < 30°$. The determination of the cell dimensions was repeated continuously in the early stages. The exposure time was recorded by a clock which ran when the X-ray window-shutter was open. About half an hour was necessary for one cycle of the determination of the accurate cell dimensions. After 6 days when the change became slow, the cell determination was done once a day.

Crystal data in the initial stage are as follows: $C_{19}H_{29}N_5O_4Co$; fw 464.48; monoclinic; a = 8.665 (2) Å, b = 13.485 (3) Å, c = 9.584 (3) Å, β = 96.95 (3)°; V = 1111.6 (5) Å^3; Z = 2; d_{measd} = 1.388 g·cm^{-3}, d_{calcd} = 1.388 g·cm^{-3}; μ = 8.79 cm^{-1}; systematic absences, $0k0$ when $k = 2n + 1$; space group $P2_1$.

Figure 2 shows the changes of a, b, c, β, and V with the exposure time. These values converged gradually to 8.637 (2), 13.833 (3), 9.539 (2) Å, 99.07 (3)°, and 1125.5 (4) Å^3, respectively. After 22 days the changes were within the experimental errors. The space group $P2_1$ remained unaltered.

The three-dimensional intensity data were collected at the stages denoted as A, B, C, D, E, F, and G in Figure 2. In the course of the data collection, the orientation matrix was redetermined if the intensities of three monitor reflections were significantly (greater than 8σ) changed. Reflections in the range of $2\theta \leq 50°$ were measured by $\omega/2\theta$ scan, a scanning rate of 8° (2θ) min^{-1}, and a scan range of $(1.0 + 0.35 \tan \theta)°$. Stationary background counts were accumulated for 5 s before and after each scan. The reflections with $|F_o| \geq 3\sigma(|F_o|)$ were used for the structure determination. No corrections for the absorption and extinction were made.

The crystal structure at the stage of A has already been reported.[5] The structure at the other stages were refined by the full-matrix least squares with the program LINEX starting from the parameters of the structure at the former stage. The refinement was made with anisotropic and isotropic thermal factors for nonhydrogen and hydrogen atoms, respectively. The hydrogen atoms of the cyanoethyl group and its disordered one could not be located in the difference map and are not

(1) (a) Tokyo Institute of Technology. (b) Niigata College of Pharmacy.
(2) Ohashi, Y.; Sasada, Y.; Tashiro, Y.; Takeuchi, S.; Ohgo, Y.; Yoshimura, J. *Bull. Chem. Soc. Jpn.* **1973**, *46*, 2589–2590.
(3) Ohashi, Y.; Sasada, Y. *Bull. Chem. Soc. Jpn.* **1977**, *50*, 1710–1715.
(4) Ohashi, Y.; Sasada, Y. *Bull. Chem. Soc. Jpn.* **1977**, *50*, 2863–2869.
(5) Ohashi, Y.; Sasada, Y.; Takeuchi, S.; Ohgo, Y. *Bull. Chem. Soc. Jpn.* **1980**, *53*, 627–634.
(6) Ohashi, Y.; Sasada, Y.; Takeuchi, S.; Ohgo, Y. *Bull. Chem. Soc. Jpn.* **1980**, *53*, 1501–1509.
(7) Ohgo, Y.; Takeuchi, S.; Yoshimura, J. *Bull. Chem. Soc. Jpn.* **1971**, *44*, 283–285.
(8) Ohgo, Y.; Takeuchi, S.; Yoshimura, J. *Bull. Chem. Soc. Jpn.* **1971**, *44*, 583.
(9) Takeuchi, S.; Ohgo, Y.; Yoshimura, J. *Chem. Lett.* **1973**, 265–266.
(10) Ohgo, Y.; Takeuchi, S.; Natori, Y.; Yoshimura, J. *Chem. Lett.* **1974**, 33–36.
(11) Ohgo, Y.; Natori, Y.; Takeuchi, S.; Yoshimura, J. *Chem. Lett.* **1974**, 709–712.
(12) Ohgo, Y.; Natori, Y.; Takeuchi, S.; Yoshimura, J. *Chem. Lett.* **1974**, 1327–1330.
(13) Yanagi, K., Master thesis, Tokyo Institute of Technology, 1981.
(14) Ohashi, Y.; Sasada, Y. *Nature (London)* **1977**, *267*, 142–144.
(15) Ohashi, Y.; Sasada, Y.; Ohgo, Y. *Chem. Lett.* **1978**, 457–460.
(16) Ohgo, Y.; Takeuchi, S.; Natori, Y.; Yoshimura, J.; Ohashi, Y.; Sasada, Y. *Bull. Chem. Soc. Jpn.* **1981**, *54*, in press.

0002-7863/81/1503-5805$01.25/0

Table I. The Average Values of the Cell Dimensions in the Course of Intensity Data Collections, the Numbers of the Reflections Used for the Structure Determinations, the Occupancy Factors of C(20), and the Final R Values at Stages A, B, C, D, E, F, and G

	A	B	C	D	E	F	G
a, Å	8.659	8.657	8.652	8.649	8.639	8.633	8.638
b, Å	13.524	13.607	13.647	13.743	13.785	13.803	13.833
c, Å	9.583	9.571	9.567	9.551	9.547	9.547	9.537
β, deg	97.16	97.70	97.93	98.48	98.73	98.85	99.06
V, Å^3	1113.4	1117.3	1118.8	1122.9	1123.8	1124.1	1125.4
N^a	1940	1879	1875	1889	1884	1893	1898
ρ^b	0.000	0.210	0.318	0.473	0.466	0.500	0.500
R	0.055	0.067	0.061	0.065	0.061	0.063	0.054

[a] The number of reflections. [b] The occupancy factor.

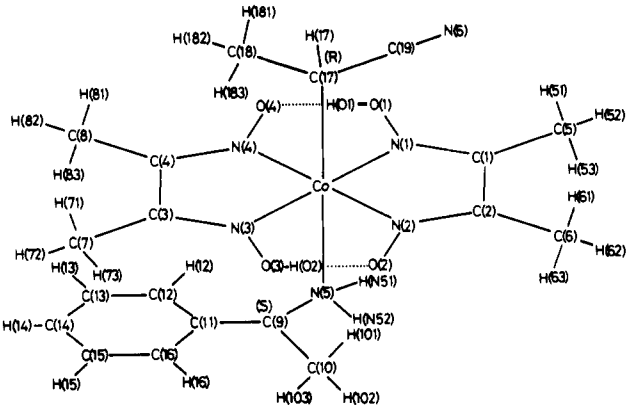

Figure 1. [(*R*)-1-Cyanoethyl][(*S*)-(−)-α-methylbenzylamine]cobaloxime.

included in the least-squares calculation. The occupancy factors of the methyl carbon atoms of the disordered cyanoethyl group, the original C(18) and newly appeared C(20), were refined. The other atoms of the disordered cyanoethyl group could not be resolved and refined as anisotropic thermal motion. The weighting scheme of $w = (\sigma(|F_o|)^2 + 0.0016|F_o|^2)^{-1}$ was employed. No peaks higher than 0.3 e Å^{-3}, except the extra peak around the cobalt atom, were found in the final difference map in each stage. The atomic scattering factors were taken from ref 17. Table I shows the average values of the cell dimensions in the course of the intensity data collection, the number of the reflections used for the structure determination, the occupancy factor of C(20), and the final R value in each stage. Atomic coordinates for the final G stage are given in Table II.[18]

For the experiments at low temperatures, the nitrogen gas-flow method was used. The unit-cell dimensions at the initial stage were determined at 133, 173, 193, 223, and 273 K. The change of the cell dimensions by X-rays was observed at 223 K. The three-dimensional intensity data at the initial stage were collected at 173 K, and its structure was analyzed, which has already been reported.[5] The experimental details were the same as those at 293 K.

The ESR spectra were obtained with Varian E-12 spectrometer by using several crystals in a capillary. For differential scanning calorimetry (DSC), the powdered sample of 6.1 mg was set in a Du Pont Instrument 990 thermal analyzer. The temperature was raised from 113 to 423 K (near the melting point) at the rate of 5 K/min, the sensitivity being 0.2 mcal.

Some difficulty in selecting the crystals at the initial stage was encountered. Even if the fractional crystallization was done several times and the optical rotation of the solution before the crystallization showed the maximum value, the crystals sometimes had the cell dimensions characteristic of the intermediate stages in Figure 2. The cell dimensions differed from crystal to crystal. For one such crystal, the structure was the same as that of the X-ray irradiated crystal with the identical cell dimensions in Figure 2. The change in cell dimensions was also brought about by room light, although the rate of the change is very small. The initial values of the cell dimensions described above are those of the crystal with the minimum unit-cell volume thus far obtained.

Results and Discussions

Electron Density Calculation. The three-dimensional intensity data were collected at the stages A, B, C, D, E, F, and G in Figure

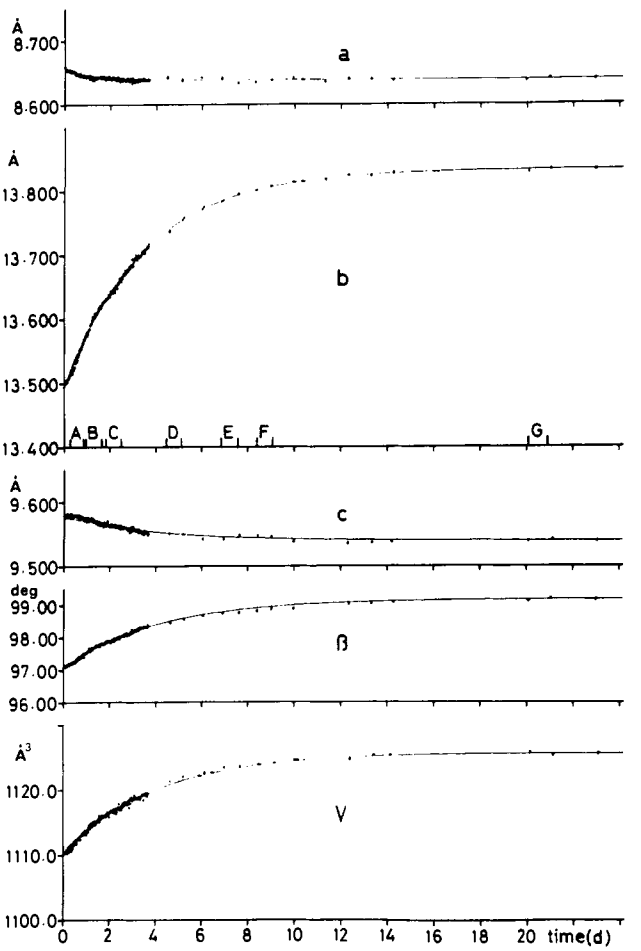

Figure 2. The change of the unit-cell dimensions. First-order reaction curves are obtained by the least-squares fitting using the observed values.

2. Significant changes in electron density were observed only in the vicinity of the cyanoethyl group. Parts a and b of Figure 3 show the composite electron density maps of the cyanoethyl group viewed along the normal to the average plane of the cobaloxime moiety at the stages A and B, respectively. Peaks of the methyl group and the carbon atom bonded to the cobalt atom, C(18) and C(17), respectively, became lowered and expanded at the stage B. Figure 3c shows a composite difference electron density map for the stage B. There appears a trough at the position of the methyl group and a peak in a neighborhood of the methyl group. Parts d, e, f, and g of Figure 3 are composite difference electron density maps at stages C, D, E, and F, respectively. The new peak grows higher and the trough becomes deeper. The composite electron density map at the final stage G is shown in Figure 3h. The height of the new peak is approximately the same as that of the original methyl carbon atom.

These observations indicate that the cyanoethyl group is becoming disordered. The position of the new peak corresponds approximately to that expected for the methyl group when the absolute configuration of the cyanoethyl group is converted from

(17) "International Tables for X-Ray Crystallography"; The Kynoch Press: Birmingham, 1974; Vol. IV, pp 72–150.

(18) See paragraph at end of paper regarding supplementary material.

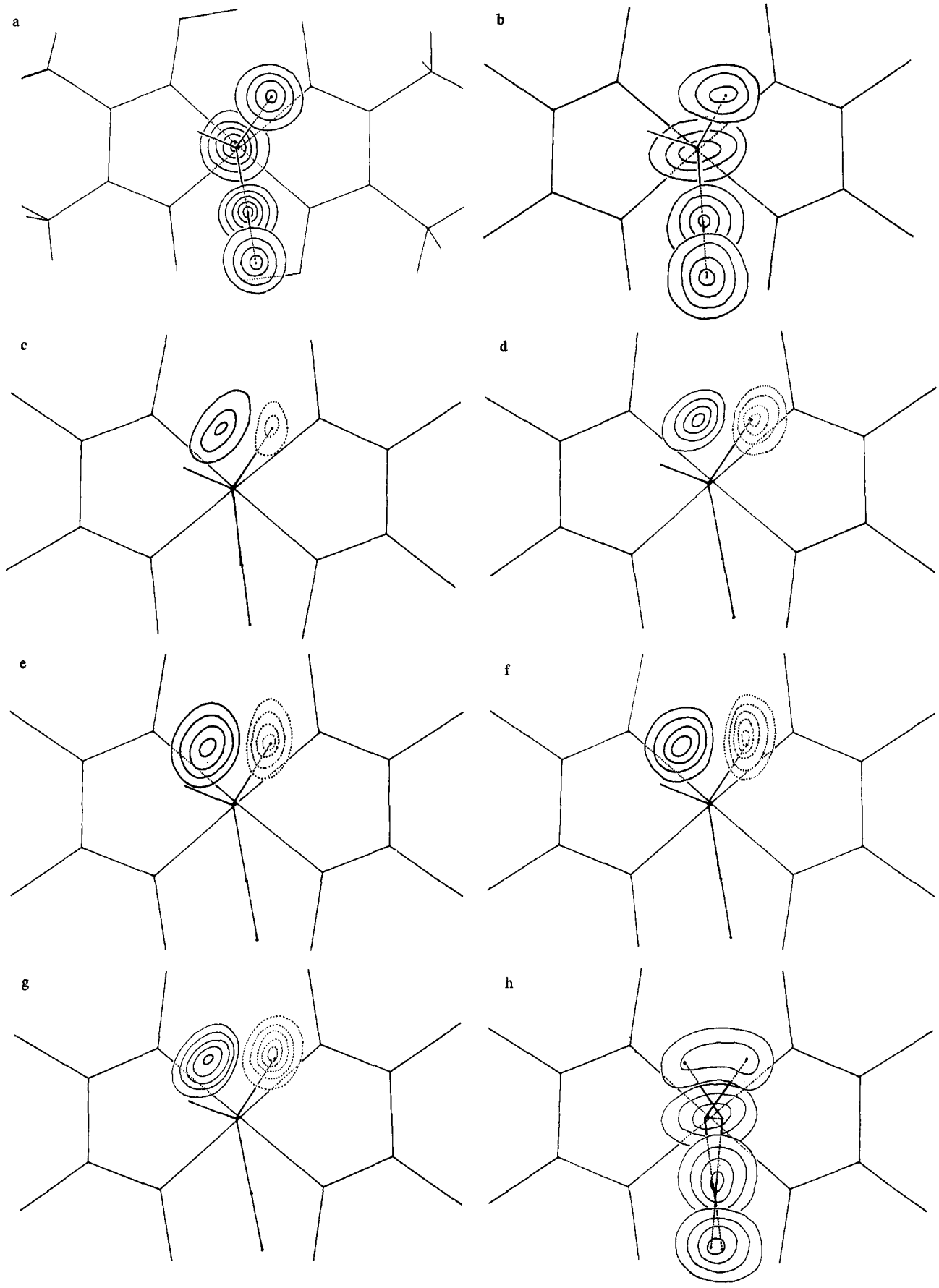

Figure 3. a and b. The composite electron density maps of the cyanoethyl group viewed along the normal to the average plane of cobaloxime at the stages A and B, respectively. Those of the other atoms are omitted for clarity. Contour interval is 1 e $Å^{-3}$. c–g. The composite difference electron density maps of the cyanoethyl group viewed along the same direction. The contour interval is 0.2 e $Å^{-3}$. In F_c calculation, the C(20) atom is excluded and the occupancy factor of the C(18) atom is altered to be 1.0. h. The composite electron density map of the cyanoethyl group at the final stage G. The expanded peaks suggest the disordered structure drawn in the figures.

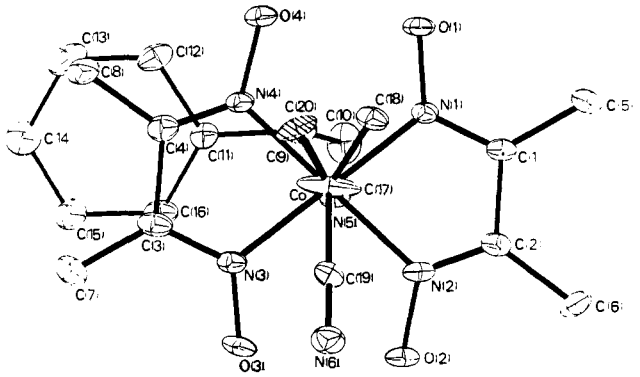

Figure 4. Molecular structure at the final stage G. The thermal ellipsoids are drawn at 30% probability. The hydrogen atoms are omitted for clarity.

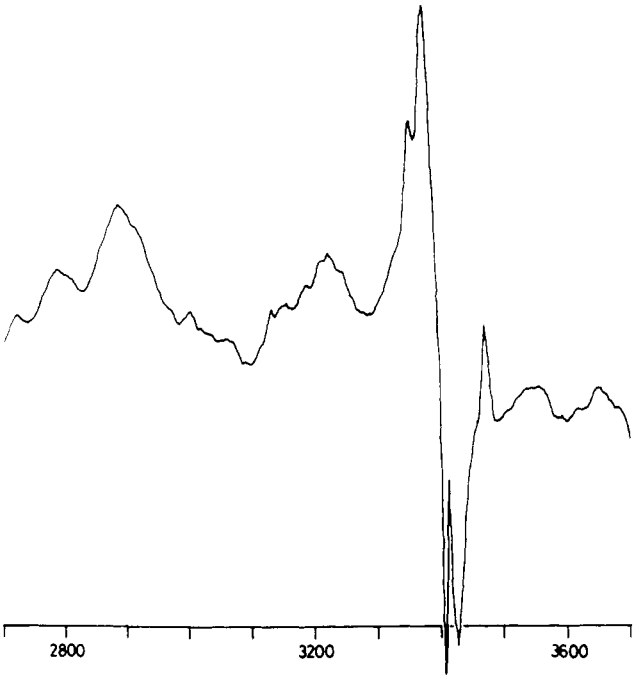

Figure 5. ESR spectra after the X-ray irradiation for 30 min. Magnetic field is plotted in the bottom (gradations 100 G) [modulation amplitude 10 G; microwave power 50 mW; microwave frequency 9.513 GHz; receiver gains 5.0×10^3]. The resonance spectrum of $g = 2.000$ is diminished in this condition owing to saturation.

R to S with the cyano group fixed. The disordered locations of the (R)- and (S)-cyanoethyl groups are indicated in Figure 3h. The least-squares calculation showed that the occupancy factors of the R and S methyl group became equal at the final stage G. Figure 4 shows the molecular structure at the final stage G. The disordering of the C(17) atom is represented by its unusually large anisotropic thermal parameters. No significant changes were observed in other bond distances and angles between the structures at the stages A and G.

ESR Spectra. Conversion of the asymmetric carbon atom of R configuration to S implies that one or more of the four bonds, Co–C, NC–C, H_3C–C, and H–C, are cleaved by X-rays in the transition state. The homolytic cleavage of the Co–C bond in alkyl(pyridine)cobaloxime complexes has been extensively studied from ESR measurement in solution.[19-22] It has been proposed that the cleavage of the Co(III)–C bond could proceed through

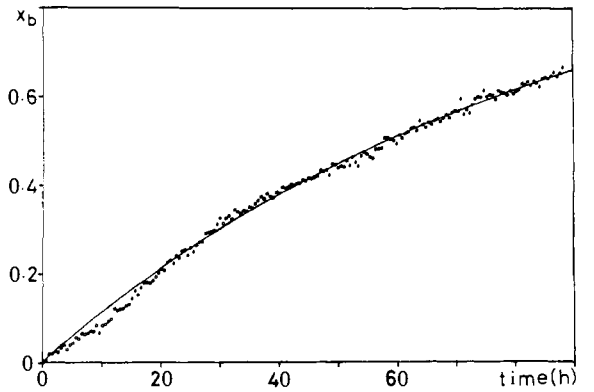

Figure 6. The normalized change of b, x_b, against the exposure time in the early stages. The curve indicates the theoretical first-order kinetics with the rate constant of 3.28×10^{-6} s^{-1}.

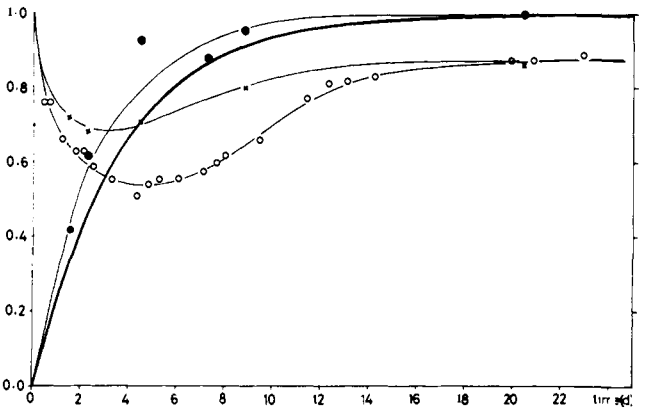

Figure 7. The changes of the occupancy factors of C(20) (a black dot) which is multiplied by 2 and averaged I_t^{int}/I_i^{int} (a cross) and I_t^{peak}/I_i^{peak} (a circle) values against the exposure time. The fine curves are drawn to fit the observed values. A thick curve is theoretical one of x_b.

the intermediate Co(II)–C bond formed by an initial electron transfer from the equatorial ligand and that if the Co(II)–C bond is weak, then the cleavage would occur.[22] The homolytic cleavage depends strongly on the nature of the alkyl group, solvent and also temperature.[22]

In order to examine whether or not the similar Co–C bond cleavage could be observed for the present crystal, ESR spectra were taken in the crystalline state before and after the X-ray irradiation. Figure 5 shows the ESR spectra after the crystal was irradiated by X-rays for 30 min. A sharp resonance was obtained in the free radical region. The g value was calculated to be 2.000. It seems adequate to ascribe it to the cyanoethyl radical compared with the related spectra in solution by Giannotti et al.[19-22] The spectra due to the Co(II) species are observed around it, although the central part is concealed by the resonance. These results may suggest that the Co–C bond is cleaved homolytically by X-ray exposure to produce the cyanoethyl radical and the Co(II) complex in the crystal.

Reaction Rate and Defects in the Crystal. The changes of a, b, c, β, and V with the exposure time are shown in Figure 2. The values of b, β, and V increase whereas those of a and c decrease with time. For comparison, it is convenient to normalize them. Figure 6 plots x_b, the normalized change of b, against the exposure time ($x_b = (b_t - b_i)/(b_f - b_i)$, where b_t, b_i, and b_f are the values at t and at initial and final stages, respectively). Normalized changes for the other parameters, x_a, x_c, x_β, and x_V, have approximately the same feature as x_b but fluctuate to a considerable extent since the magnitude of the total changes for a, c, β, and V are less than that for b.

The plot seems to be approximate first-order kinetics. The rate constant, k_b, was calculated to be 3.28×10^{-6} s^{-1}. The theoretical curves are drawn in Figure 6 and also in Figure 2. However, the

(19) Giannotti, C.; Bolton, J. R. *J. Organomet. Chem.* **1974**, *80*, 379–383.
(20) Giannotti, C.; Merle, G.; Fontaine, C.; Bolton, J. R. *J. Organomet. Chem.* **1975**, *91*, 357–362.
(21) Giannotti, C.; Merle, G.; Bolton, J. R. *J. Organomet. Chem.* **1975**, *99*, 145–156.
(22) Giannotti, C.; Bolton, J. R. *J. Organomet. Chem.* **1976**, *110*, 383–388.

Table II. Atomic Coordinates for the G Stage

atom	*x/a*	*y/b*	*z/c*	B_{eq},[a] Å²
Co	0.0075 (1)	0.2500	0.2695 (1)	3.9
N(1)	0.1666 (6)	0.1551 (4)	0.2922 (6)	4.3
N(2)	0.0122 (6)	0.2232 (4)	0.4639 (5)	4.7
N(3)	−0.1542 (6)	0.3434 (4)	0.2446 (6)	4.8
N(4)	0.0046 (6)	0.2775 (4)	0.0758 (5)	4.8
O(1)	0.2416 (5)	0.1270 (4)	0.1855 (5)	5.2
O(2)	−0.0904 (6)	0.2616 (5)	0.5413 (5)	6.6
O(3)	−0.2387 (6)	0.3641 (4)	0.3458 (5)	6.3
O(4)	0.1035 (5)	0.2337 (4)	−0.0034 (5)	5.3
C(1)	0.2039 (7)	0.1182 (6)	0.4173 (7)	4.9
C(2)	0.1109 (8)	0.1587 (6)	0.5200 (7)	4.8
C(3)	−0.1866 (8)	0.3811 (5)	0.1197 (8)	5.2
C(4)	−0.0917 (8)	0.3436 (5)	0.0184 (8)	5.3
C(5)	0.3281 (10)	0.0430 (7)	0.4544 (10)	6.7
C(6)	0.1249 (9)	0.1227 (8)	0.6706 (8)	7.1
C(7)	−0.3187 (10)	0.4499 (6)	0.0754 (9)	6.7
C(8)	−0.1044 (12)	0.3758 (6)	−0.1325 (8)	6.9
N(5)	−0.1629 (6)	0.1422 (4)	0.2342 (6)	5.1
C(9)	−0.2032 (8)	0.0878 (5)	0.1003 (7)	5.0
C(10)	−0.2860 (12)	−0.0077 (7)	0.1310 (10)	7.8
C(11)	−0.3036 (8)	0.1439 (5)	−0.0124 (7)	5.1
C(12)	−0.4406 (8)	0.1896 (6)	0.0071 (8)	5.2
C(13)	−0.5349 (8)	0.2364 (7)	−0.1015 (8)	6.6
C(14)	−0.4912 (10)	0.2356 (12)	−0.2362 (9)	8.6
C(15)	−0.3641 (11)	0.1895 (10)	−0.2609 (9)	9.0
C(16)	−0.2681 (9)	0.1433 (7)	−0.1514 (9)	6.9
C(17)	0.1715 (10)	0.3560 (7)	0.3197 (10)	7.4
C(19)	0.1349 (9)	0.4151 (6)	0.4368 (9)	6.1
N(6)	0.1082 (9)	0.4655 (6)	0.5196 (8)	8.9
C(18)	0.3309 (18)	0.3404 (15)	0.3075 (23)	8.4
C(20)	0.2757 (42)	0.3933 (20)	0.2482 (31)	14.6

atom	*x/a*	*y/b*	*z/c*	*B*, Å²
H(O1)	0.142 (7)	0.183 (6)	0.034 (8)	6 (2)
H(O2)	−0.162 (9)	0.299 (6)	0.468 (8)	9 (2)
H(51)	0.332 (8)	0.010 (7)	0.533 (8)	9 (2)
H(52)	0.406 (10)	0.076 (7)	0.425 (9)	12 (3)
H(53)	0.320 (11)	−0.003 (8)	0.400 (9)	11 (3)
H(61)	0.025 (9)	0.096 (7)	0.680 (9)	10 (2)
H(62)	0.108 (9)	0.175 (7)	0.709 (8)	9 (2)
H(63)	0.228 (7)	0.132 (5)	0.708 (6)	5 (2)
H(71)	−0.363 (8)	0.472 (6)	0.163 (7)	7 (2)
H(72)	−0.268 (8)	0.511 (6)	0.072 (7)	7 (2)
H(73)	−0.386 (7)	0.441 (5)	−0.003 (7)	6 (2)
H(81)	−0.105 (7)	0.443 (5)	−0.151 (7)	6 (2)
H(82)	−0.165 (8)	0.336 (6)	−0.202 (8)	9 (2)
H(83)	−0.043 (10)	0.362 (7)	−0.184 (9)	9 (2)
H(N51)	−0.150 (6)	0.085 (5)	0.289 (6)	5 (2)
H(N52)	−0.249 (12)	0.175 (9)	0.268 (11)	14 (3)
H(9)	−0.098 (6)	0.077 (4)	0.084 (6)	4 (1)
H(101)	−0.346 (9)	0.005 (8)	0.195 (8)	10 (2)
H(102)	−0.204 (8)	−0.045 (6)	0.202 (7)	7 (2)
H(103)	−0.307 (10)	−0.049 (7)	0.031 (9)	10 (3)
H(12)	−0.469 (7)	0.178 (5)	0.100 (6)	6 (2)
H(13)	−0.647 (7)	0.276 (6)	−0.085 (6)	6 (2)
H(14)	−0.555 (8)	0.266 (7)	−0.317 (8)	9 (2)
H(15)	−0.338 (7)	0.185 (5)	−0.343 (7)	6 (2)
H(16)	−0.175 (9)	0.120 (7)	−0.147 (9)	10 (3)

[a] B_{eq} means the equivalent isotropic temperature factor.

curve shows a sigmoidal region in the stages between 0 and 50 h. This indicates that the racemization of the cyanoethyl group proceeds cooperatively in the early stages. The rate constants of the other dimensions, k_a, k_c, k_β, and k_V, were calculated in the same way as k_b. They are 3.41×10^{-6}, 2.95×10^{-6}, 2.82×10^{-6}, and 2.86×10^{-6} s^{-1}, respectively. The sigmoidal nature for other parameters were not so clear as *b*.

The occupancy factors of the newly appeared methyl carbon, C(20), at the B–G stages were calculated in the least-squares refinement. They are plotted against the exposure time in Figure 7, in which the first-order change of x_b is also shown. The curve fitted to the occupancy factors are slightly higher than that for x_b. However, the former curve approached the latter one when the occupancy factors were calculated in the condition that the *R* and *S* methyl groups should have identical isotropic temperature

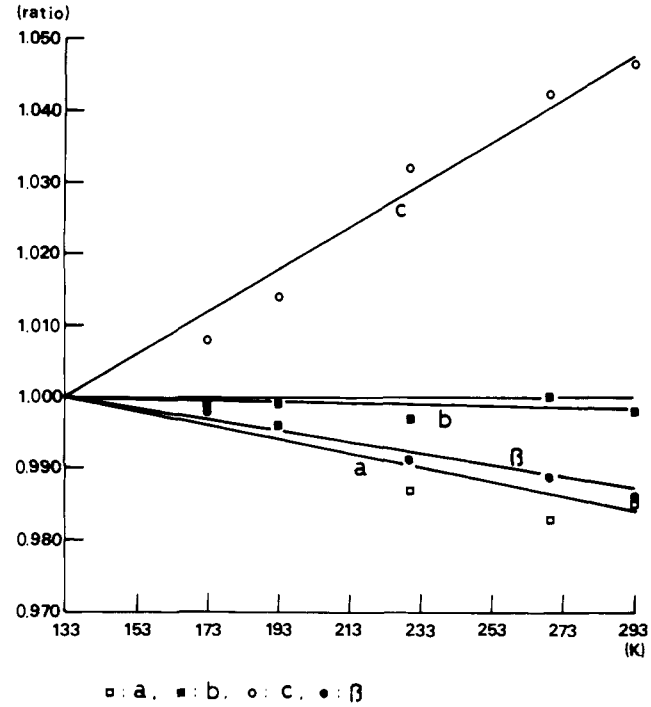

Figure 8. The change of the unit-cell dimensions with temperature. Each value is normalized by the corresponding one at 133 K [8.791 (2) Å, 13.516 (2) Å, 9.161 (2) Å, and 98.31 (3)° for *a*, *b*, *c*, and *β*, respectively].

factors in the least-squares refinement. Therefore, it is adequate to consider that the change of x_b is a good indicator for the degree of the racemization of the cyanoethyl group and the racemization proceeds in the first-order kinetics.

The peak and integrated intensities of reflections varied to a considerable extent, although the appearance of the crystal gave no evidence of decomposition or degradation. The peak and integrated intensities at each stage were normalized against their initial values, I_t^{peak}/I_i^{peak} and I_t^{int}/I_i^{int}, respectively. They were averaged for five reflections, which had strong intensities and the least variation in the F_c calculation for the structures from A to G stages. The averaged values of I_t^{peak}/I_i^{peak} and I_t^{int}/I_i^{int} are plotted against the exposure time in Figure 7.

The averaged value of I_t^{int}/I_i^{int} decreased rapidly by about 30% at the early stages and then increased slowly and turned to 88% the initial value. If the periodic structure of the crystal were strictly conserved during the X-ray exposure, the integrated intensities might be approximately constant at every stage, judged from the fact that the structural change, as a whole, is small. The decrease in the integrated intensities is probably due to the defects arising during the reaction. The defects reached a maximum after 3 days and did not disappear at the final stage, considered from the variation curve of the averaged I_t^{int}/I_i^{int}.

The averaged value of I_t^{peak}/I_i^{peak} decreased rapidly by 50% after about 5 days and recovered at approximately the same ratio as that of the integrated intensities. Because the peak intensity is the weighted sum of the two reflections brought about by the original and racemate cells, it should become a minimum when the number of the original and racemate cells are equal ($x_b = 0.5$). And at the final stage the averaged value of I_t^{peak}/I_i^{peak} would be equal to that of I_t^{int}/I_i^{int}, since all the cells have changed to the racemate cells. The recovery of the peak intensities seems to be retarded by the defects formed in the crystal.

Change at Low Temperatures. When the crystal was cooled below 173 K, the gradual change of its unit-cell dimensions by X-ray exposure was no longer detectable. The values of *a*, *b*, *c*, *β*, and *V* at 173 K are 8.786 (2) Å, 13.500 (2), Å, 9.243 (2) Å, 98.09 (3)°, and 1085.5 (4) Å^3, respectively. Because their changes from the values at 293 K were very characteristic, the unit-cell dimensions were measured at several temperatures. Each value showed an approximately linear change with temperature as shown in Figure 8. In view of experimental error, there were no dis-

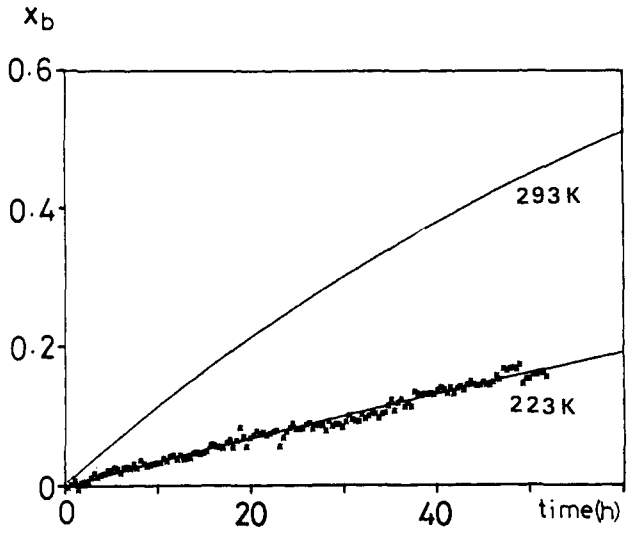

Figure 9. The change of x_b at 223 K against the exposure time. The upper curve is the theoretical one of x_b at 293 K.

continuous changes of cell dimensions with temperature. This is consistent with the result of the thermal analysis, which did not show any endothermic or exothermic transition between 113 and 423 K. The linear coefficients of thermal expansion were derived to be -1.00×10^{-4}, -0.10×10^{-4}, and 2.95×10^{-4} K^{-1} for a, b, and c, respectively. Since the cell dimensions varied with the X-ray exposure near room temperature, it was impossible to determine whether or not the change depending on temperature is reversible.

The change of the cell dimensions with the exposure time was observed at 223 K. It showed a similar characteristic but a significantly slower rate compared to the change at 293 K. The normalized change of b at 223 K is plotted against the exposure time in Figure 9, in which the first-order reaction curve at 293 K is also drawn. The change at 223 K obeys first-order kinetics, and the rate constant, k_b, was derived to be 0.98×10^{-6} s^{-1}, which is about one-third of that obtained at 293 K. The sigmoidal change observed at 293 K was less pronounced at 223 K.

Structural Difference between 173 and 293 K. The crystal structures at 173 and 293 K at the initial stage A have already been reported.[5] The atoms in the neighborhood of the cyanoethyl group together with short interatomic distances at 293 K are shown in Figure 10. They belong to the cobaloxime moiety or the amine ligand and not to the cyanoethyl group of the neighboring complexes. The cyano group makes close contacts with the complex at $(-x, {}^1/_2 + y, 1 - z)$. The nitrogen atom of the cyano group forms a weak hydrogen bond of N···H–N with the neighboring amine. The methyl group has the usual van der Waals contacts with the neighboring complex along the a axis but fairly loose contacts along the b and c axes. The H(17) atom makes no direct contacts with the complex related by 2_1 symmetry. The interatomic distances of H(17)···H(103), H(17)···H(16), and H(182)···H(103) are 3.05, 2.79, and 3.43, respectively. There appears to be a void around H(17).

When the crystal is irradiated by X-rays, the transferred methyl group of S configuration, C(20), fills up the void around H(17). However, the void is not large enough to accommodate the methyl group so that the crystal must expand along the 2_1 axis, b axis, as the racemates grow. If the crystal is cooled, it contracts to a great extent along the c axis. The complex at $(-x, {}^1/_2 + y, -z)$ approaches that at (x, y, z), the direction of shift being parallel to the c axis so that the void around H(17) disappears. The interatomic distances of the initial structures at 173 and 293 K and of the racemic structure are listed in Table III. Although the bond distances and angles are not significantly different between the structures at 173 and 293 K, a slight rotation around the Co–N(5) bond, 3.4°, is found between the two structures. This also contributes the close packing around H(17). These results well explain the slow reaction rate at low temperatures and inhibition of the racemization of the cyanoethyl below 173 K.

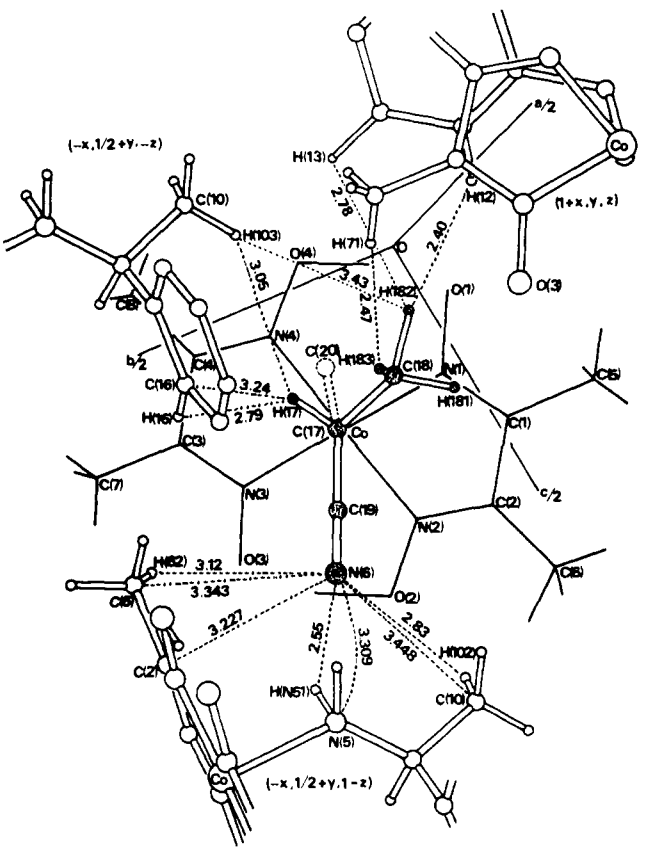

Figure 10. The atoms in the neighborhood of the cyanoethyl group viewed along the normal to the average plane of cobaloxime of the original position and the short interatomic distances at 293 K. The shaded atoms are those of the cyanoethyl group in the original unit. The coordinates in parentheses indicate the equivalent positions.

Table III. The Short Interatomic Distances at 173 and 293 K and at the Final Stage G[a]

atom	atom	position	dist, Å 173 K	293 K	G stage
C(19)	C(6)	III	3.561 (8)	3.664 (12)	3.689 (14)
C(19)	H(62)	III	2.56 (7)	3.28 (7)	2.98 (10)
N(6)	C(2)	III	3.242 (8)	3.227 (11)	3.262 (12)
N(6)	C(6)	III	3.386 (8)	3.343 (12)	3.305 (14)
N(6)	H(62)	III	2.57 (7)	3.12 (7)	2.74 (10)
N(6)	N(5)	III	3.218 (7)	3.309 (10)	3.371 (11)
N(6)	H(N51)	III	2.34 (5)	2.55 (7)	2.45 (7)
N(6)	C(10)	III	3.438 (8)	3.448 (12)	3.462 (14)
N(6)	H(102)	III	2.76 (6)	2.83 (7)	2.65 (8)
C(18)	O(3)	II	3.789 (8)	3.728 (12)	3.693 (23)
H(182)	H(12)	II	2.97 (7)	2.40 (12)	
H(182)	H(13)	II	2.85 (9)	2.78 (13)	
H(183)	H(71)	II	2.54 (7)	2.47 (11)	
H(17)	H(103)	I	2.47 (8)	3.05 (10)	
H(17)	H(16)	I	2.53 (9)	2.79 (8)	
H(182)	H(103)	I	2.56 (8)	3.43 (12)	
C(20)	C(10)	I			3.882 (38)
C(20)	C(16)	I			3.578 (38)
C(20)	H(103)	I			2.83 (10)

[a] Equivalent positions I, II and III are $-x$, ${}^1/_2 + y$, $-z$, $1 + x$, y, z, and $-x$, ${}^1/_2 + y$, $1 - z$, respectively.

Reaction Mechanism. The void around H(17) explains the capability of the racemization of the cyanoethyl group in the crystalline state. In order to examine the void more precisely, we have defined the cavity for the cyanoethyl group as the concave space limited by the envelope surface of the spheres, whose centers are positions of inter- and intramolecular atoms in the neighborhood of the cyanoethyl group, the radius of each sphere being greater by 1.2 Å than the van der Waals radius[23] of the corre-

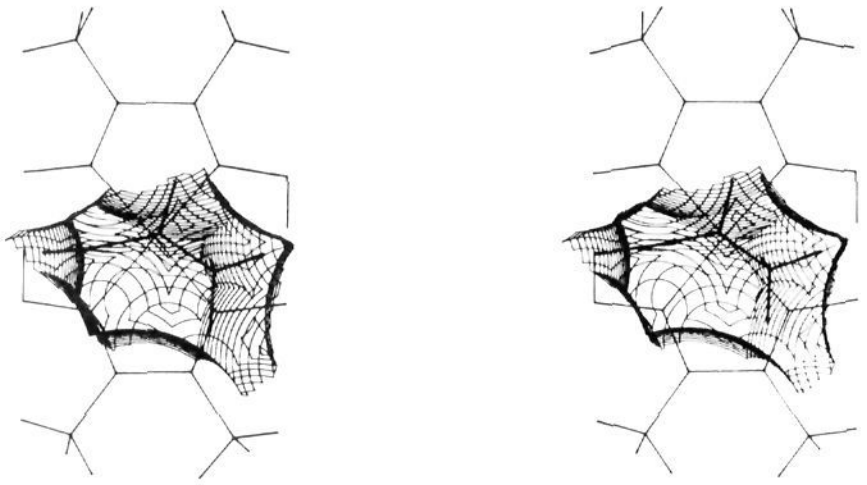

Figure 11. A stereoscopic drawing of the cavity for the cyanoethyl group of the initial structure at 293 K. The contours are drawn in sections separated by 0.10 Å.

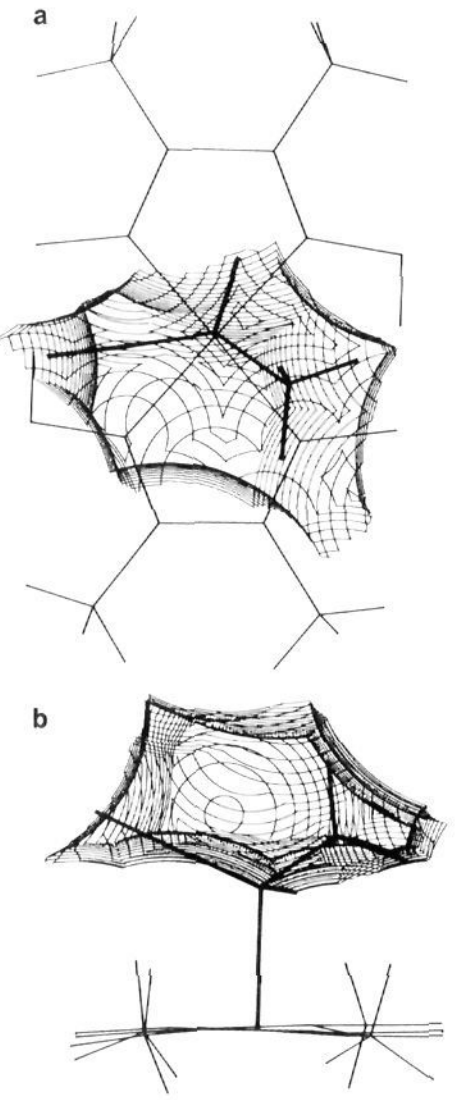

Figure 12. The cavity for the cyanoethyl group of the structure at 293 K viewed along (a) the normal to the average plane of cobaloxime and (b) the long axis of cobaloxime. The contours are drawn in sections separated by 0.10 Å.

sponding atom. Any point in the cavity is then considered to be accessed by the centers of atoms of the cyanoethyl group.

Figure 11 shows a stereoscopic drawing of the cavity of the initial structure at 293 K. In order to compare the cavity with those of other stages, it is convenient to draw its projections along two orthogonal axes, one of which is normal to the cobaloxime plane and another is along the long axis of the cobaloxime. Figures 12 and 13 illustrate the cavities of the initial structures at 293 and 173 K, respectively. Figure 14 shows the cavity of the final structure at 293 K. The three cavities are compared in Figure 15, in which the cobaloxime moiety is fixed in the same position. One can easily notice the void around H(17), part A in Figure 15a, which is filled up with the transferred methyl group. There is another void space near the methyl group, part B in Figure 15a, in the initial structure at 293 K. The void also disappears in the final racemate structure. It appears that void B is transferred and added to void A as the racemates grow.

(23) Bondi, A. *J. Phys. Chem.* **1964**, *68*, 441–451.

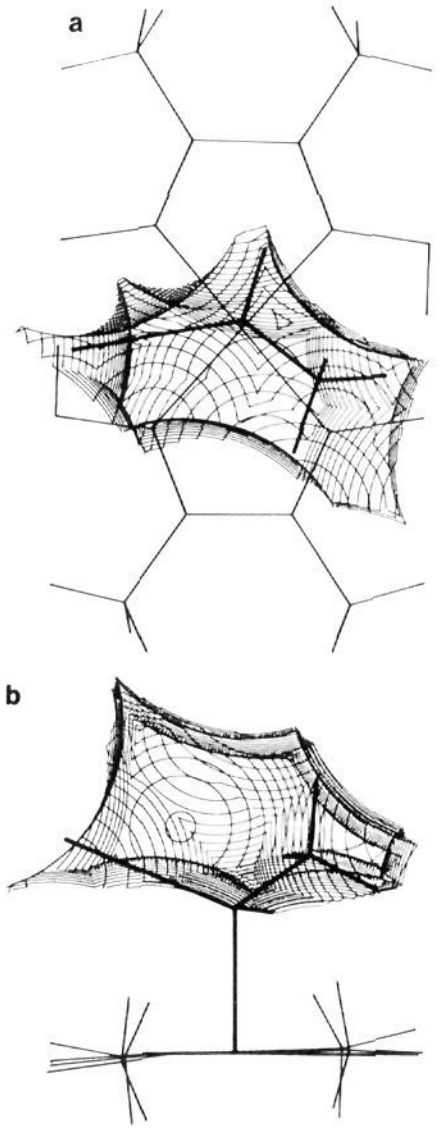

Figure 13. The cavity for the cyanoethyl group of the structure at 173 K drawn in the same way as Figure 12.

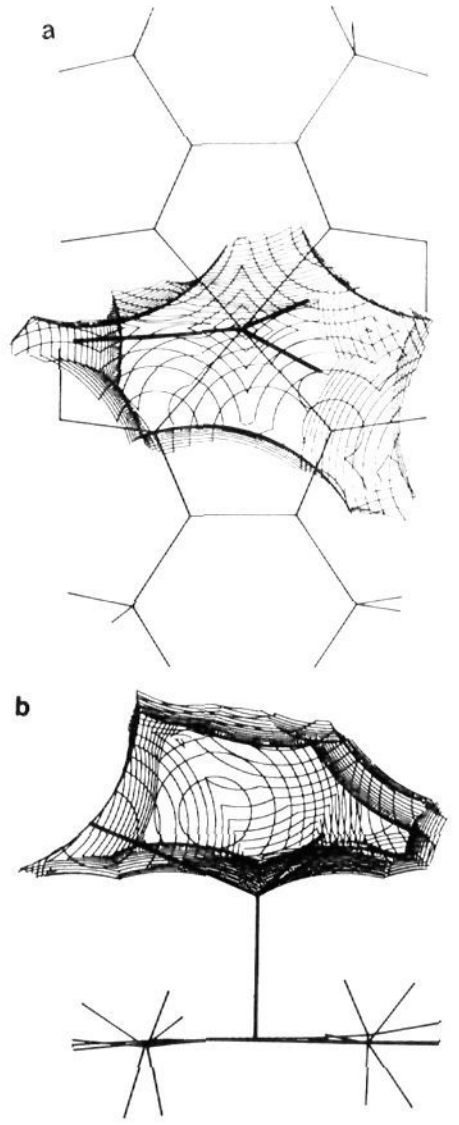

Figure 14. The cavity for the cyanoethyl group of the final G stage structure at 293 K drawn in the same way as in Figure 12.

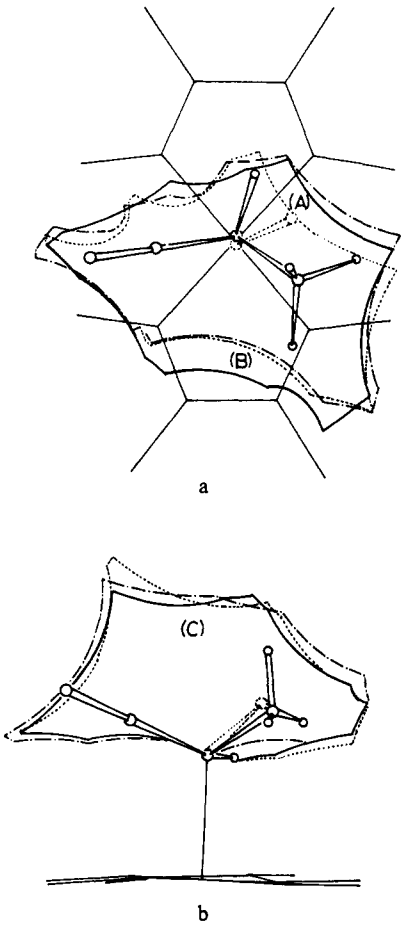

Figure 15. Comparison of the three cavities. The solid, dotted, and dot and dashed curves indicate the peripheries of the cavities at 293 and 173 K and at the final stage G, respectively. A, B, and C are void spaces observed in the structure of the initial stage A at 293 K. The dotted circle indicates the C(20) atom.

The volume of each cavity was calculated by the summation of the volumes allotted to the grid points in the cavity, the mesh of the points being decreased step by step until the constant value was obtained. The cavities at 293 and 173 K have the volume of 14.53 and 12.95 Å^3, respectively, and that of the final structure is 15.24 Å^3. If the cavity is assumed to be a cube in the first approximation, the space occupied by the cyanoethyl group is considered as a cube with a side of ($14.53^{1/3}$ + 2.4) Å in the unit cell at 293 K since the cavity has a space of 1.2 Å in width around it. Therefore, the change of the cavity in volume brought about by lowering temperature or by X-ray exposure, 1.58 or 0.71 Å^3, respectively, corresponds to the decrease of 6.21 Å^3 or the increase of 2.83 Å^3 in the volume of the unit cell. The corresponding changes of a complex are 13.1 and 7.0 Å^3, respectively, which are derived from the cell change. The corresponding ratios of the changes for the cyanoethyl group to those for the complex, therefore, are 0.47 and 0.40, respectively, which are as about twice as the volume ratio (0.20) of the cyanoethyl group (113.4 Å^3) to the complex (555.8 Å^3). This appears to be a favorable condition for the crystalline state reaction.

Besides voids A and B, there is another void space above the cyanoethyl group, part C in Figure 15b, which remains at the low temperature. This void space seems to be very advantageous to the racemization of the cyanoethyl group because the Co–C bond should be cleaved by X-rays and the formed cyanoethyl radical should change to the cyanoethyl group with the opposite configuration. The final but fundamental question remains unsolved; how the cyanoethyl group with the opposite configuration is formed from the cyanoethyl radical? One possible explanation may be the rotation of the cyanoethyl radical around the C—C≡N bond. Void space C may suggest the explanation. The cavity is too small for the rotation, but the energy released by the Co–C recombination may reinforce the thermal motion of the neighboring complex, translational and librational, to bring about instantaneously a wide space enough for the rotation.

Once a racemate is formed, the growth of the racemic structure would continue since the racemic structure is apparently more stable thermodynamically than the original one. On account of almost identical cell dimensions and crystal structures of the enantiomer and racemate, a whole crystal is converted into the disordered structure without destroying a single crystal form.

Acknowledgment. We are grateful to Dr. T. Yamase for assistance in obtaining ESR spectra and helpful discussion, and to Prof. S. Seki and Prof. H. Suga for assistance in obtaining DSC data and valuable discussion.

Supplementary Material Available: Tables of the observed and calculated structure factors and the anisotropic temperature factors at the stage G and tables of positional and thermal parameters and the observed and calculated structure factors at the stages B–F (53 pages). Ordering information is given on any current masthead page.